Shape memory nanocomposite fibers for untethered high-energy microengines

Jinkai Yuan, Wilfrid Neri, Cécile Zakri, Pascal Merzeau, Karl Kratz, Andreas Lendlein, Philippe Poulin

Shape Memory Polymer Fibers for High-Energy Torsional Actuators

Jinkai Yuan[1, *], Wilfrid Neri[1], Cécile Zakri[1], Pascal Merzeau[1], Karl Kratz[2], Andreas Lendlein[2], Philippe Poulin[1, *]

[1]Centre de Recherche Paul Pascal, CNRS, Université de Bordeaux, 115 Avenue Schweitzer, 1033600 Pessac, France.

[2]Institute of Biomaterial Science and Berlin-Brandenburg Center for Regenerative Therapies, Helmholtz-Zentrum Geesthacht, 14513 Teltow, Germany

*Correspondence to: yuan@crpp-bordeaux.cnrs.fr
poulin@crpp-bordeaux.cnrs.fr

We report thermally powered torsional actuators using shape memory polymer fibers that provides unique performances. These torsional actuators can generate rotation per length on the order of 4000 turns/m. The gravimetric torque generation capabilities of the fibers are more than 21 N.m/kg, over three times higher than that of electric motors. The twisted shape memory fibers combine high torque with large angles of rotation, delivering a gravimetric work capacity as high as 2766 J/kg, which is 60 times higher than nature skeletal muscles. Its distinctive temperature memory twist capability adds additional advantage over conventional torsional actuators by allowing for the tunability of the operation temperature. The use of the twisted shape memory fiber as a motor to propel a boat is demonstrated.

Miniature torsional actuators are of practical interest for emerging applications, ranging from microrobotics, lab-on-a-chip technology, smart textiles, to micro-electromechanical systems and miniaturized medical devices (*1*). Fuel-powered or electromagnetic rotating engines are classical torsional actuators, generally used to provide fast and large torsional actuation on the macroscale. However, it is difficult to miniaturize and integrate them into micro-devices due to their weight and complex design.

Making large-stroke, high-speed, high-energy miniaturized torsional actuators with simplicity and robustness remains challenging. Different materials and mechanisms have been sought for over a century to provide torsional actuation, such as shape memory alloy (*2*), piezoelectric ceramics (*3*) and electroactive polymers (*4*). The simplest form of easily implementable small scale torsional actuator is certainly the rubber band elastomer used in airplane toys (*5*) . However, such type of actuators need to be hooked and have a very low energy density related to the low Young's and shear moduli of elastomers. Nevertheless, the most promising torsional actuators reported up to now are still based on the concept of twisted fibers (*6*). The insertion of the twist dramatically amplifies the strokes and work capacities compared with those for nontwisted or noncoiled fibers.

Since the first demonstration of electrochemically driven torsional actuators based on twist-spun carbon nanotube (CNT) yarns in 2011 (*7*), a new class of actuating materials, highly twisted and coiled CNT yarns, has emerged and been extensively investigated in past years (*6*). The helical topology enables a conversion of the yarn volumetric expansion into tensile contraction and torsional untwist, delivering gravimetric work capacities on the order of 10^3 J/kg for the best systems (*8-10*). The volume change has been driven by the expansion of infiltrated guest materials

in response to heat (*8, 11*), liquid adsorption (*9, 10*), or by the surface tension of liquids diffused through multiscale gaps of hierarchically arranged helical CNT fibers (*12, 13*).

Although highly twisted CNT yarns provide interesting actuation performances, the difficulty and high cost of fabricating these CNT muscles has restricted their applications. By contrast, simple and low-cost artificial muscles can be made by twisting polymer fibers that are widely available and capable of deforming in response to large temperature changes because of thermal expansion. For instance, upon raising temperature by ~140 °C, twisted nylon-6,6 fibers contract and untwist, generating a torsional energy density as high as ~2100 J/kg (*14*), which represents the state of the art for artificial muscles. In fact, besides thermal expansion, twisted polymer fibers can be actuated in torsion based on other mechanisms, such as entropic elasticity of polymer chains (*5*) and electrostatic attraction between cylindrical electrodes in buckled sheath-core rubber muscles (*15*). Here, we show that twisted polymer fibers can operate via shape memory mechanisms to act as torsional actuators.

In twisted shape memory fibers, the polymer chains are frozen in helically configured deformation below a thermal transition temperature. The torsional actuation is simply triggered by a temperature change above the temperature of the involved thermal transition. The shape memory torsional actuation is shown to provide large stroke at high rotation rate, giant energy density for small temperature variation operation. Actually, using semi-crystalline polymers with reinforced shear moduli, we demonstrate unprecedented energy density of 2766 J/kg for a temperature raise of only a few degrees Celsius (from a few degrees below the transition to a temperature slightly above the transition). The present torsional actuators don't have to be hooked making their use and implementation particularly easy. The combination of mechanical simplicity, record energy

density, low cost and micrometer-size fiber diameter make the present technology readily implementable in applications that require rotation in microdevices or smart textile structures.

Torsional actuation of shape memory polymer fibers

We start from semi-crystalline polyvinyl alcohol (PVA) fibers with low cost but high strength and high toughness (*16, 17*), reflecting their capability of absorbing large amounts of mechanical energy. Such type of materials have been shown to be efficient as thermally-powered shape memory actuators in the mode of linear elongation and contraction (*16*). Here, we explore the potential of wet-spun PVA fibers as shape memory torsional actuators. They are promising candidates because they combine high thermal stability and large flexibility. In addition, the scalable wet-spinning process allows for a large tunability of tensile and torsional stiffness by incorporating various nanoparticles to provide enhanced work capacity.

A 2-cm-long, 40-μm-diameter raw PVA fiber (**Fig. 1A**) was first heated up to 100°C (above the glass transition temperature, T_g ~80°C). Isobaric (in condition of constant tensile force provided by a weight attached at the fiber end) twist was then inserted into this fiber in 7500 turns per meter of fiber length, with a rotation speed of 60 revolutions per minute (rpm). Unless otherwise noted herein, the inserted twist is in isobaric condition. Afterwards, the twisted fiber was quenched to room temperature to fix the formed coiling structure (**Fig. 1B**). All the previously reported coiled CNT yarns (*8*), polymer fibers (*14*) or rubber bands (*5*) are torque balanced to prohibit torsional rotation of the coiled yarns before being stimulated to act as muscles. By contrast, the coiled structure of shape memory fibers can be retained without being hooked because of the frozen nonequilibrium conformation of the twisted polymer chains. Upon reheating the programmed fiber up to a high temperature (above T_g), the one end tethered fiber rotated its free end to revert toward its original and equilibrium shape via untwist (**Fig. 1C**). A practical example of the programming

and torsional actuation of the twisted fiber in response to heat is shown in Movie S1. By contrast to the mechanism of thermal expansion, which requires large changes of temperature, the torsional actuation is here triggered by a thermal transition which can be tuned by changing the type of shape memory polymer used (*18*).

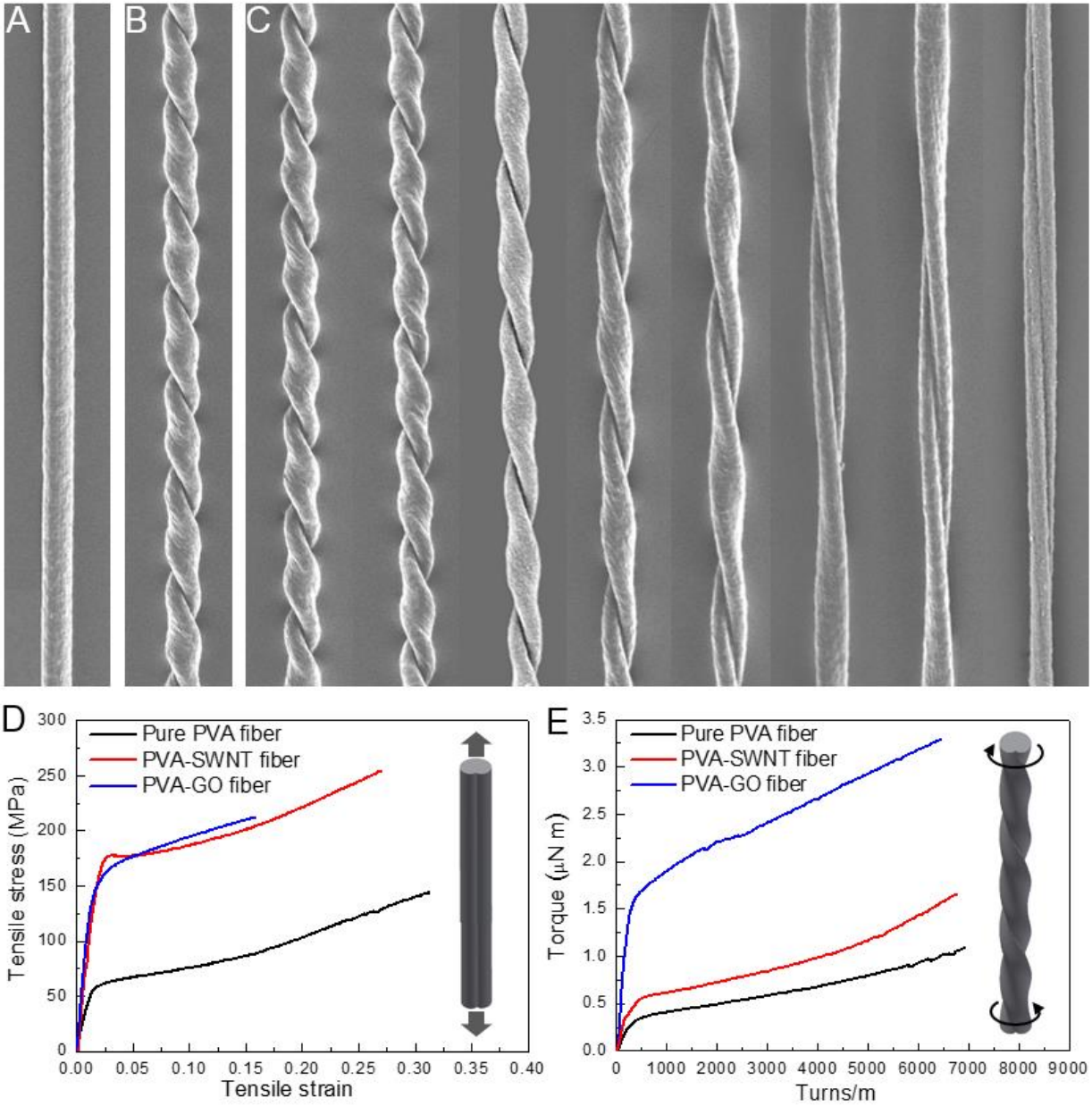

Fig. 1. Shape memory polymer fibers for torsional actuators. (**A**) The scanning electron microscope (SEM) of a 40-μm-diameter PVA fiber. Its cross-sectional morphology is shown in Fig. S1. (**B**) The SEM image of coiled PVA fiber, which was achieved by inserting a twist at

T_d~100°C, followed by quenching in the air. This temporary coiled structure can be conserved at room temperature and does not need to be hooked. (**C**) The evolution of morphology of twisted fiber as it untwisted in response to the reheating in an oven from room temperature to a high temperature above T_g. (**D**) Tensile stress versus strain curves at room temperature for pure PVA fibers and PVA composite fibers reinforced respectively with 5 wt.% SWNT and 5 wt.% GO nanoparticles. (**E**) The torque needed to twist the neat PVA, PVA-SWNT and PVA-GO fibers until their rupture at room temperature. The quantitative measurements of the torque and applied twist angle were obtained by using home-made instruments (Fig. S2). The detailed characterizations are described in the section method of Supplementary Information. The curves of shear stress versus shear strain at low strain levels are given in Fig. S3, which allows for the comparison of shear modulus of different fibers.

The energy that an actuator provides via shape recovery is a growing function of the energy absorbed during the twist program at a high temperature, T_d. It is expected that the polymer can be made stronger, and therefore more efficient for high-energy-density actuation by the inclusion of reinforcing nanofillers. We prepared single wall carbon nanotube (SWNT)- and graphene oxide (GO)-doped PVA fibers by using wet-spinning method upon injection of a PVA-SWNT dispersion or PVA-GO solution in an aqueous solution of Na_2SO_4 as coagulating bath(*17*).

Quantitative characterizations were achieved by measuring the stress or torque needed to respectively stretch or twist the fibers. As shown in **Fig. 1D**, the neat PVA fiber shows high toughness and a tensile Young's moduli as high as 4.9 GPa. The incorporation of SWNT or GO nanosheets slightly decreases the strain to failure but largely improves the tensile strength by increasing the Young's moduli up to 13.5 GPa and 12.5 GPa respectively. More importantly it raises the toughness, which is the mechanical energy absorbed by the fiber, represented by the area under the tensile curve. Both nanofillers have nearly the same reinforcement efficiency on the tensile properties. By contrast, a much greater torque is needed to twist the PVA-GO fiber to a given angle compared to neat PVA or PVA-SWNT fibers (**Fig. 1E**). By assuming the fiber as a rigid elastic cylinder, the shear stress and strain can be calculated at small twist angles before the onset of coiling (Fig. S3). The SWNT and GO nanoparticles boost the shear moduli (~1.3 GPa) of

PVA fiber up to 2.3 GPa and 6.8 GPa, showing an improvement of 177% and 523% respectively. Relative to SWNTs, GO nanosheets have a more significant effect on the improvement of torsional properties because of their two-dimensional structure. As schematically illustrated in Fig. S4, these nanosheets allow the fiber to sustain a tensile stress by the deformation in tension, as for SWNTs, but also a high torque under shear. The strong PVA-GO fibers are therefore chosen to investigate in more depth the torsional actuation of shape memory fibers.

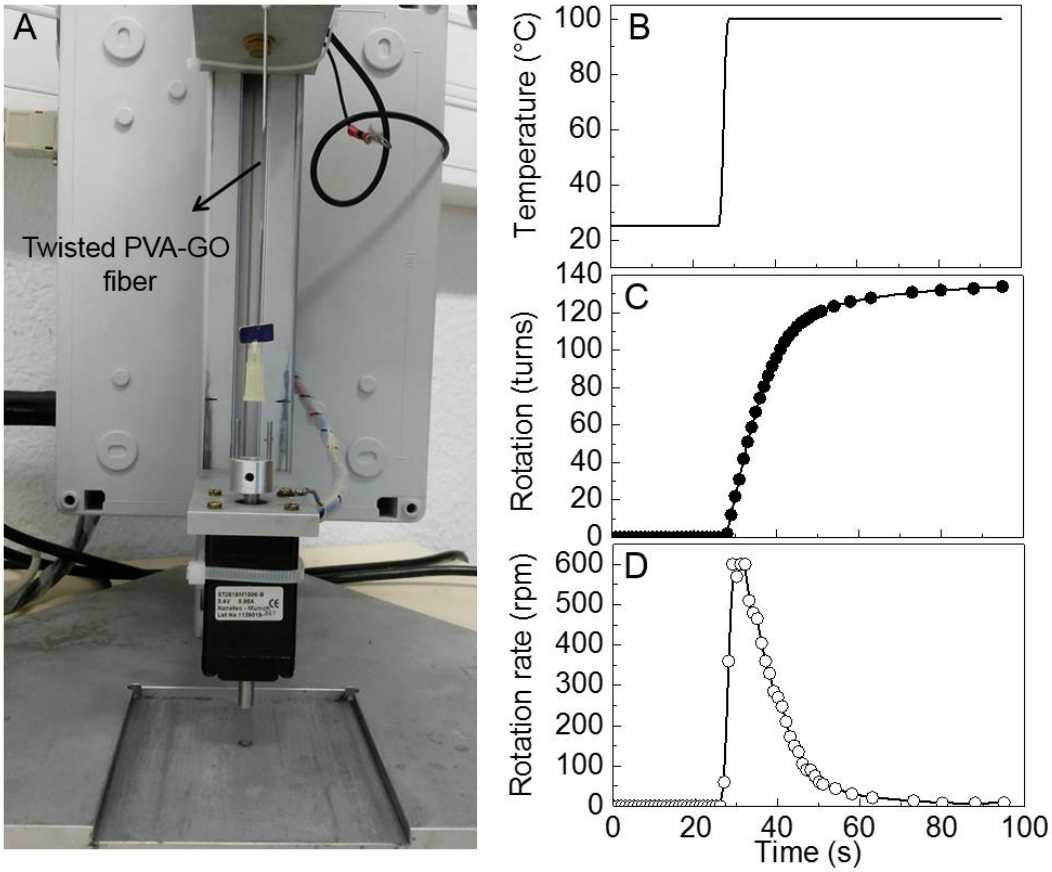

Fig. 2. Free rotation of shape memory torsional actuators in response to heat. (**A**) The programmed fiber was achieved by twisting a 3-cm-long, 40-μm-diameter PVA-GO fiber by 225 turns at 80°C, which was followed by quenching at room temperature to fix the twisted deformation. (**B**) Temperature variation in the twisted fiber as a result of the immediate heating in an oven. **(C)** The rotation versus time achieved using frame-by-frame analysis of Movie S2. (**D**) Rotation rate in rpm was calculated based on the first derivative of the curve of rotation versus time in (C).

Fast torsional actuation was quantitatively demonstrated for a one end tethered, twisted PVA-GO fiber (**Fig. 2A**). Upon immediate heating from room temperature to 100°C in an oven (**Fig. 2B**), the fiber rotated at the free end a 5000 times heavier syringe needle and a paper paddle, which was recorded by a high-speed camera (Movie S2). The rotation versus time is obtained using frame-by-frame analysis and shown in **Fig. 2C**. The whole rotation process contains 134 full turns. The torsional stroke reaches 4467 turns/m. This is the highest value ever reported for torsional actuators to the best of our knowledge. This value is 6.4 times higher than electrochemically driven CNT yarn muscles (694 turns/m) (*7*), more than twice of the GO hydrogel fiber based torsional actuators (1635 turns/m) (*19*), two or three orders of magnitudes higher than that achievable in other actuators based on buckled sheath-core fibers (13 turns/m) (*15*), twisted nylon-6,6 fibers (14.4 turns/m) (*14*), and paraffin wax infiltrated niobium nanowires (33 turns/m) (*20*). Detailed comparisons with more actuators can be found in Table S1.

The first derivative of rotation versus time curve gives the rotation rate (**Fig. 2D**). The paddle was accelerated to a peak rotation rate of 600 rpm in 2 s and maintained for ~5 s and ~50 full rotations. This peak rotation rate compares with the electrochemically powered CNT yarn muscles (*7*) but is lower than other torsional actuators based on twisted niobium nanowires (*20, 21*), GO hydrogel fibers (*19*), and guest filled CNT yarns (*8, 11*). It should be noted that, for shape memory actuating fibers, the torsional rotation angle and rate can be optimized or tailored by changing the heating rate, the temperature variation operation, the inserted twist per meter of fiber length and, as detailed below, even the programming temperature. Additionally, as thermally powered shape memory actuator, the twisted fiber can be principally triggered to untwist by any kind of heating manner. In addition to the oven, a practical example of heating the fiber in viscous silicon oil is demonstrated in Movie S3.

Temperature memory of twisted polymer fibers

The effect of programming temperature, T_d, on the torsional actuation was investigated for PVA-GO fibers with a length of 3 cm and a diameter of 40 μm. **Fig. 3A** shows the torque needed to twist the fibers up to 7500 turns/m at different T_d. The absorbed mechanical energy is estimated from the area under each curve. A greater torque is needed to twist the fibers at a lower T_d, indicating that more torsional mechanical energy is stored during program. As shown in **Fig. 3B**, when reheating the fiber in free load conditions from room temperature to 185°C at a rate of 5°C/min, higher full rotations are generated for fibers that have been initially programmed at lower T_d. A maximum value of 6123 turns/m was recorded by varying the temperature ~160°C. The fibers that have been twisted at greater T_d recover partially their shape at higher temperatures but show decreased full rotations. The rate of recovery decreases with increasing the programming temperature. The best recovery rate is obtained for a recovery temperature near T_g.

Based on the first derivative of the curve of rotation versus time (Fig. S5), the rotation rate can be calculated and plotted as a function of temperature in **Fig. 3C**. The twisted fiber untwists with a peak rate at a well-defined temperature, which is equal to T_d in each case, showing a temperature memory effect, closely reminiscent of temperature memory effects previously observed in tension or contraction (*16*).

Instead of calculating the start-up torque ($\tau = Ia$) that accelerates a paddle with a moment of the inertia, I, at an acceleration, a. Here, thanks to our home-made instrument (Fig. S2), we are able to directly measure the generated torque upon reheating the programmed fiber at fixed deformation from room temperature to 220 °C at a rate of 5 °C/min. The fiber programmed at 100 °C generated the maximum gravimetric torque ~21 Nm/kg (**Fig. 3D**), which is lower than Nature's bacterial flagellar (200 Nm/kg) (*22, 23*), but much higher than previously developed artificial torsional

actuators (Table S1). Even by varying T_d far from T_g, this value decreases but still remains on the order of 10 Nm/kg, which is 5.4 times higher than that for electrochemically powered CNT yarn muscles (1.85 Nm/kg) (*7*) and two or three orders of magnitude higher than materials torsionally actuated by liquid or vapor adsorption (*12*, *13*, *19*). The present fibers can even compare with the shape memory niobium nanowires (8 Nm/kg) (*21*), guest filled twist-spun CNT yarns (8.42 Nm/kg) (*8*) and the ungeared commercial direct drive electric motors (2.5-6 Nm/kg) (*24*). Moreover, the peak of recovery torque occurs at a temperature at which that the fibers have been initialed programmed. This is another consequence of the temperature memory effect.

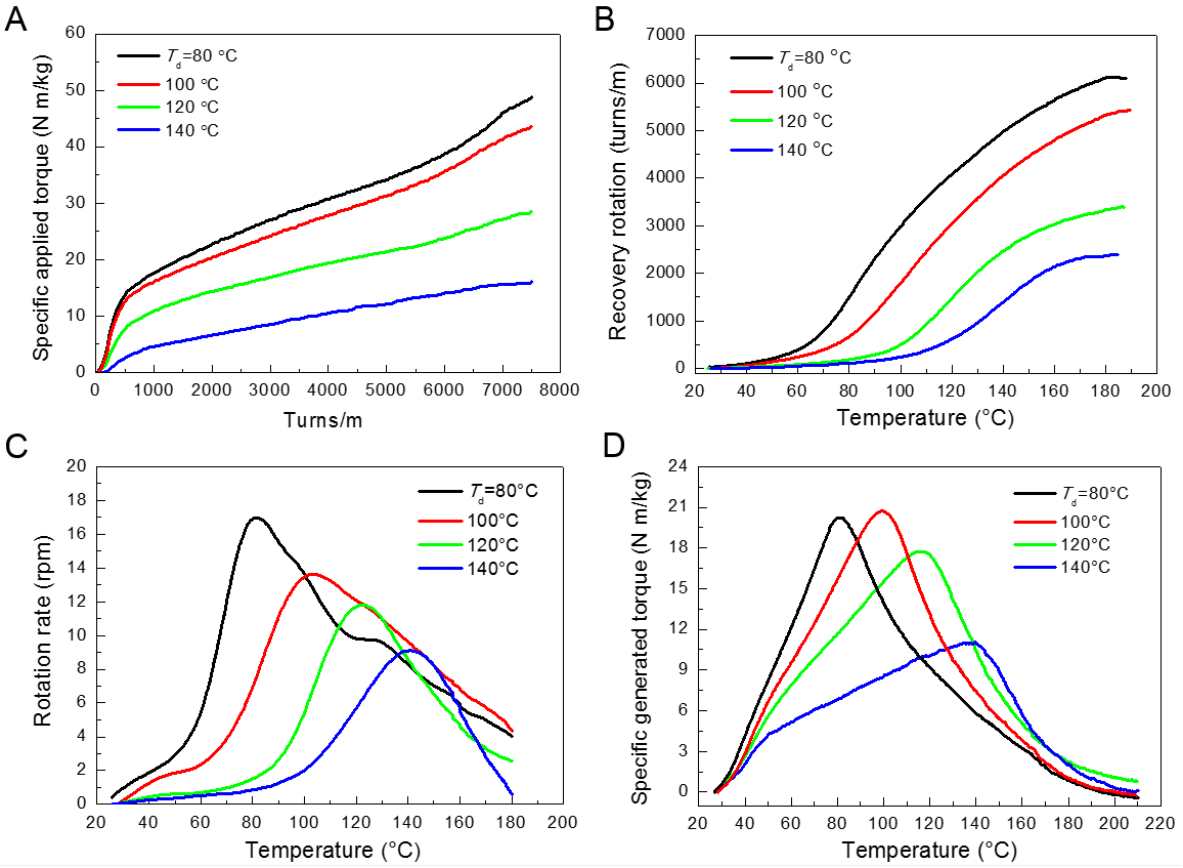

Fig. 3. Temperature memory of twisted polymer fibers. (**A**) 3-cm long, 40-μm-diameter PVA-GO fibers were programmed by inserting a twist of 7500 turns/m with a rotation rate of 60 rpm at different temperatures T_d varying from 80° to 140°C. The specific torque versus twisted angle was recorded at each temperature. (**B**) Recovery rotation with free load for the twisted fibers that are programmed at different T_d. (**C**) Evolution of rotation speed with temperature obtained by the first derivative of the curve of rotation versus time shown in Fig. S5. The peak rate appears at a

temperature equal to T_d, showing a temperature memory effect. (**D**) Specific torque generated by PVA-GO fibers when they are reheated. In this case, the coiled fiber is tethered at both ends to prevent fiber untwisting. A peak of torque is observed in each case at a temperature which is equal to T_d, demonstrating a temperature memory effect.

The distinctive feature of temperature memory, compared to other torsional actuators, allows for the rational control of the actuation without varying the chemical structure of polymer fibers to tailor T_g. This enables the actuators to be customized for releasing the stroke or torque in the vicinity of a certain temperature needed for a particular application.

High energy density of twisted shape memory fibers

In the torsion mode, the generated mechanical energy is expressed as $U = \int \Gamma d\theta$ when the fiber rotates by an angle θ against a given torque Γ. In this regard, we chose T_d ~100°C to insert a large amount (10,000 turns/m) of twist into 23-μm diameter neat PVA, PVA-SWNT, and PVA-GO fibers, which were obtained by thermally drawing the as-prepared fibers by 200%. The reduction of the fiber diameter retards the onset of coiling thus significantly increasing the amount of twist that can be inserted before the direct contact of neighboring coils(*14*). As shown in **Fig. 4A**, a greater torque is needed to twist PVA-GO fiber at T_d~100 °C as compared to neat PVA and PVA-SWNT fibers because of the unique torsional reinforcement effect of GO additives.

Quantitative characterizations of the work capacity of twisted fibers can be achieved by measuring the recovery angle against a constant torque. We first tethered the two ends of the twisted fibers that have been quenched without being hooked. Upon reheating from room temperature to 210°C at a rate of 5°C/min, the recovery torque reaches its maximum $\tau_{maximum}$ at 100°C for each fiber (**Fig. 4B**). $\tau_{maximum}$ can be viewed as a blocking torque. For PVA-GO fiber it reaches ~0.27 μN m, which is far higher than 0.12 μN m and 0.11 μN m respectively achieved

for PVA-SWNT and neat PVA fiber. Knowing the maximum torque that the fibers can generate, we then measured the recovery angle against an applied torque τ_{applied} below τ_{maximum}. The fiber untwists to provide mechanical output as the temperature increases up to a temperature operation window (ΔT, in the vicinity of T_d~100°C) in which the recovery torque remains superior to τ_{applied}. In the case of PVA-GO fiber, with increasing the applied torque from 20% to 80% of τ_{maximum}, the recovery rotation yet decreases and the needed temperature operation window ΔT becomes narrower from 120°C to 70°C (**Fig. 4C**). Such trade-off allows an optimum of gravimetric work capacity at an intermediate load. The gravimetric work capacity is defined here as the amount of work done by the fibers in rotation, divided by the mass of the fibers. **Fig. 4E** shows the accomplished gravimetric mechanical output as a function of the ratio of $\tau_{\text{applied}}/\tau_{\text{maximum}}$. It is found that, in response to a temperature variation of 100°C in the vicinity of T_d (Fig. S6), the twisted PVA-GO fiber can rotate against a load of 0.135 μN.m to provide a maximum gravimetric work capacity as high as 1800 J/kg. This energy density is far higher than mammalian skeletal muscles (39 J/kg) (*25*) and even than most of the previously reported artificial torsional actuators (Table S1) based on CNT yarns (73.2 J/kg) (*7*), helical CNT fibers (26.7 J/kg) (*12*), shape memory NiTi nanowires(0.11J/kg) (*21*), and GO hydrogel fibers (230 J/kg) (*19*). However, this energy density is 14% lower than twisted nylon-6,6 fibers muscles (2100 J/kg), which are actually operated by being torque balanced.(*14*)

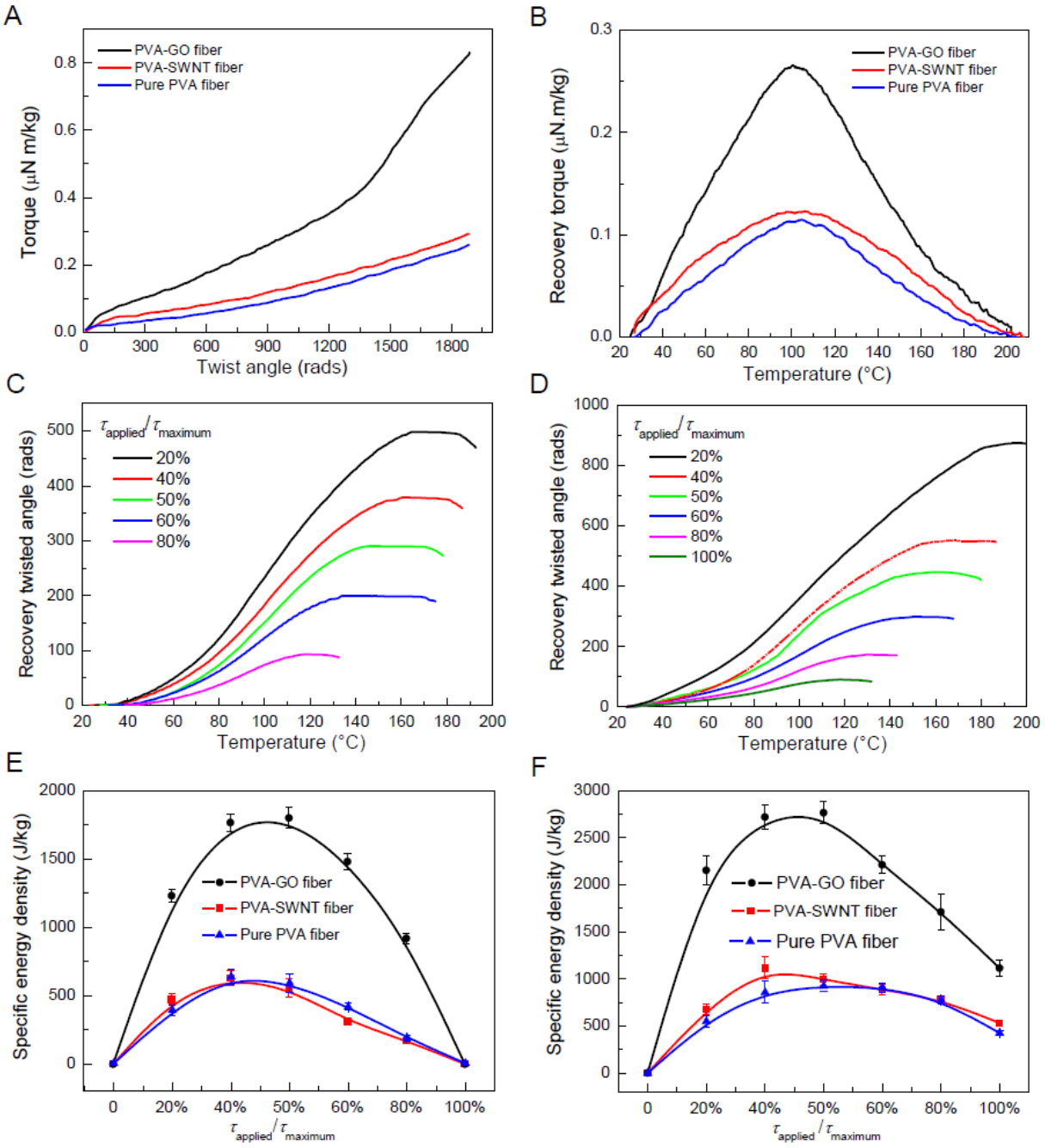

Fig. 4. High energy density of twisted shape memory fibers. (**A**) Torque needed to respectively twist 3cm-long, 23-μm diameter neat PVA, PVA-SWNT, and PVA-GO fibers by 1885 rads (10,000 turns/m) at a rate of 60 rpm at T_d ~100°C. The twisted fibers are afterwards quenched to room temperature to form coils with and without being torque balanced for the further different actuation characterizations. (**B**) Recovery torque generated by the coiled fibers that have been quenched without being hooked when they are reheated. The both ends of the fibers are tethered, and the temperature is increased from room temperature to 210°C at a rate of 5°C/min. A maximum torque $\tau_{maximum}$ occurs at 100°C with a clear peak in each case. (**C, D**) Recovery angle upon reheating in conditions of variable applied torques $\tau_{applied}$ for the programmed PVA-GO fiber.

The applied torque $\tau_{applied}$ varies from 20% to 80% of $\tau_{maximum}$ ~0.27 μN m of PVA-GO fiber. The coiled fiber rotates against the applied torque to generate mechanical output as the temperature increases from room temperature until a high temperature at which the recovery torque starts to be inferior to $\tau_{applied}$. (**E, F**) The gravimetric work capacities for different coiled fibers, which are calculated by multiplying the specific applied torque and the recovery angle against this torque. The coiled fibers used for (C, E) are formed by quenching in air without being hooked therefore losing some twist because of the partial shape fixity of our PVA based fibers. While for (D, F) the coiled fibers are quenched by balancing the twist inserted into the fibers. The hook is removed before being stimulated to rotate.

In fact, the torsional actuator based on twisted shape memory fibers can be operated in the same manner as well. Being different from highly cross-linked PVA materials (*26*), wet-spun PVA fibers can not 100% fixe the twisted deformation, which results in losing several turns of twist after temperature quench in air. By contrast, a torque balanced structure can be added to prevent such untwist and enhance further the mechanical output. The hook is immediately removed when heating of the fiber starts in order to torsionally actuate the fiber. **Fig. 4D** shows the recovery rotations against different loads for the twisted PVA-GO fibers that have been quenched and hooked. At the same load, the fibers rotate by a larger number of turns compared to twisted fibers quenched without being torque balanced (**Fig. 4C**), and thus provide a much greater gravimetric energy density of 2766 J/kg at an optimum $\tau_{applied}$~0.135 μN m (Fig. S7 and **Fig. 4F**). To the best of our knowledge, this energy density is higher than that of state of art torsional actuators based on twisted nylon-6,6 fibers (*14*).

For comparison, PVA-CNT fibers and neat PVA fibers were employed to perform exactly the same protocols to characterize their optimum energy density. Energy density of 628 J/kg and 1115 J/kg were observed for twisted PVA-CNT fibers that have been quenched without and with being torque balanced respectively (**Fig. 4E, F** and Fig. S8). While neat PVA fibers show the similar energy generation capabilities, 632 J/kg and 925 J/kg for the fibers quenched without and with

being hooked respectively (**Fig. 4E, F** and Fig. S9). These levels of energy turn out inferior to those of PVA-GO fibers but can still compare with nature skeletal muscles and some of the best torsional actuators aforementioned (Table S1).

Application

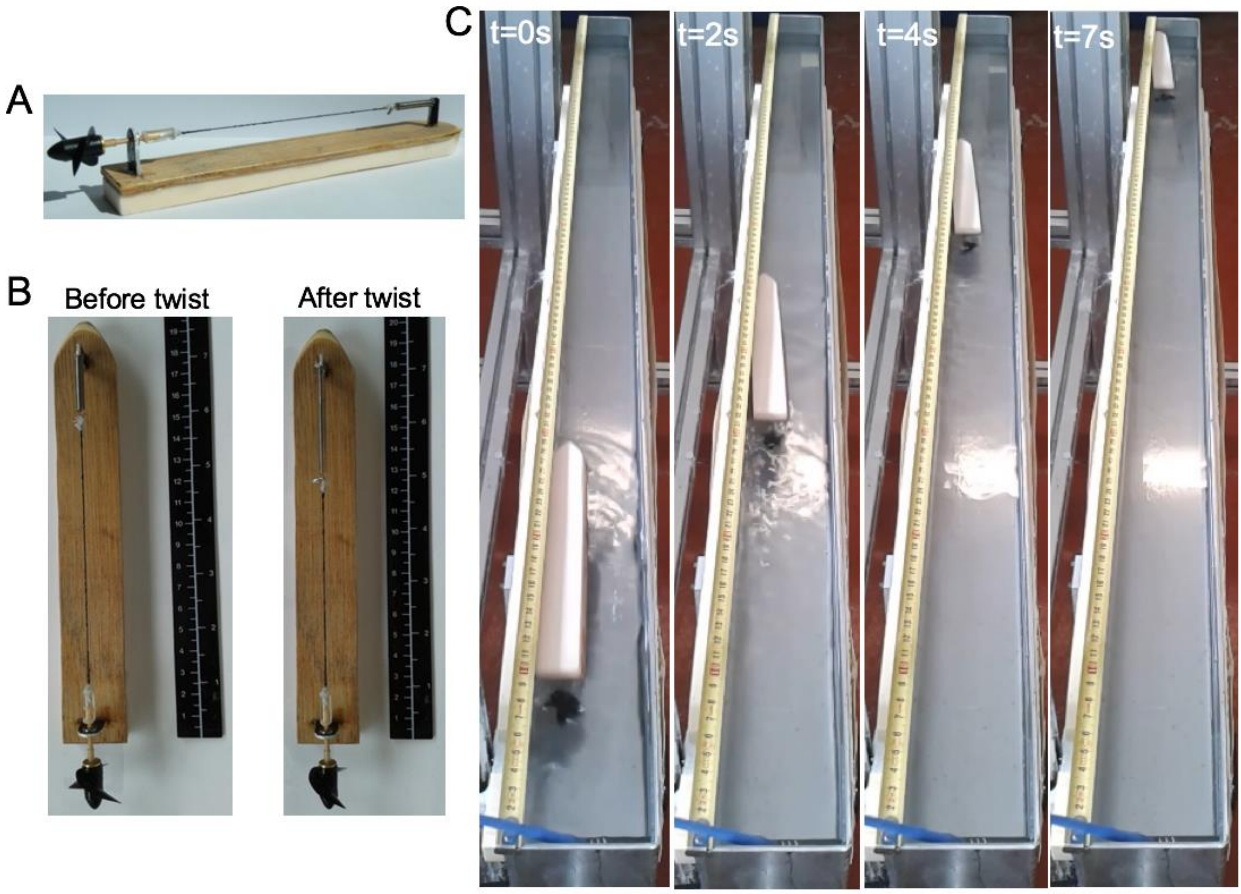

Fig. 5. Twist and navigate. (**A**) Photograph of prototype motor based on shape memory polymer fibers that can rotate the propeller for a boat. (**B**) Five 100-μm-diameter PVA-CNT fibers were plied together to form a yarn with a length of 12 cm, and this yarn was placed under a boat and connected to a spring on one end, and to a propeller on the other end. The yarn was programmed by inserting a twist of 80 turns in 100°C silicon oil, which was followed by a quench at room temperature. The twisted fiber was found to be shortened to 9.5 cm. (**C**) Images from Movie S4 show the navigation of a boat as the fiber untwists in response to the heat of the silicon oil.

We have designed and demonstrated a crude prototype of a motor for a boat based on the twisted shape memory fibers (**Fig. 5A**). To generate sufficient torque and mechanical energy, five fibers with large diameter (~100 μm) were plied together to make a twisted yarn that is stable and does not need to be torque balanced by combining twisting at 100°C and further temperature quench in air (**Fig. 5B**). Upon heating in hot silicon oil, the boat is propelled by the twisted shape memory fiber. The fiber untwists and the boat moves by one meter in only 7 seconds (**Fig. 5C** and Movie S4).

In summary, we have developed torsional actuators based on shape memory fibers that can rotate in response to a thermal transition. This transition can be triggered by a simple temperature change, at a temperature that depends on the composition of the polymer or on the programming stage (temperature memory). Based on the PVA fibers that are torsionally stiffened by the inclusion of two dimensional graphene oxide, a remarkable recovery torque with a large torsional stroke is achieved, opening opportunity to make strong torsional actuators with unprecedentedly high gravimetric work capacity. Additionally, the distinctive temperature memory feature enables a large tunability of the operation temperature. The cost, robustness, versatility and attractive actuation performances make our torsional actuators promising for demanding applications in which the microsystem can be mechanically reloaded or used at one time.

References and Notes

1. G. V. Stoychev, L. Ionov, Actuating fibers: design and applications. *ACS Appl. Mater. Interfaces* **8**, 24281-24294 (2016)
2. K. J. Gabriel, W. S. N. Trimmer, J. A. Walker, A micro-rotary actuator using shape memory alloys. *Sens. Actuators* **15**, 95-102 (1988).
3. J. Kim, B. Kang, Performance test and improvement of piezoelectric torsional actuators. *Smart Mater. Struct.* **10**, 750-757 (2001).

4. Y. Fang, T. J. Pence, X. B. Tan, Fiber-directed conjugated-polymer torsional actuator: nonlinear elasticity modeling and experimental validation. *IEEE-Asme T. Mech.* **16**, 656-664 (2011).
5. J. Yuan, P. Poulin, Fibers do the twist. *Science* **343**, 845-846 (2014).
6. C. S. Haines *et al.*, New twist on artificial muscles. *Proc. Natl. Acad. Sci. U S A.* **113**, 11709-11716 (2016).
7. J. Foroughi *et al.*, Torsional carbon nanotube artificial muscles. *Science* **334**, 494-497 (2011).
8. M. D. Lima *et al.*, Electrically, chemically, and photonically powered torsional and tensile actuation of hybrid carbon nanotube yarn muscles. *Science* **338**, 928-932 (2012).
9. M. D. Lima *et al.*, Efficient, Absorption-powered artificial muscles based on carbon nanotube hybrid yarns. *Small* **11**, 3113-3118 (2015).
10. S. H. Kim *et al.*, Bio-inspired, moisture-powered hybrid carbon nanotube yarn muscles. *Sci. Rep.* **6**, 23016 (2016).
11. K. Y. Chun *et al.*, Hybrid carbon nanotube yarn artificial muscle inspired by spider dragline silk. *Nat. Commun.* **5**, 3322 (2014).
12. P. N. Chen *et al.*, Hierarchically arranged helical fibre actuators driven by solvents and vapours. *Nat. Nanotech.* **10**, 1077-1083 (2015).
13. S. S. He *et al.*, A mechanically actuating carbon-nanotube fiber in response to water and moisture. *Angew. Chem. Int. Ed.* **54**, 14880-14884 (2015).
14. C. S. Haines *et al.*, Artificial muscles from fishing line and sewing thread. *Science* **343**, 868-872 (2014).
15. Z. F. Liu *et al.*, Hierarchically buckled sheath-core fibers for superelastic electronics, sensors, and muscles. *Science* **349**, 400-404 (2015).
16. P. Miaudet *et al.*, Shape and temperature memory of nanocomposites with broadened glass transition. *Science* **318**, 1294-1296 (2007).
17. C. Mercader *et al.*, Scalable process for the spinning of PVA-carbon nanotube composite fibers. *J. Appl. Polym. Sci.* **125**, E191-E196 (2012).
18. M. Behl, M. Y. Razzaq, A. Lendlein, Multifunctional shape-memory polymers. *Adv. Mater.* **22**, 3388-3410 (2010).
19. H. Cheng *et al.*, Moisture-activated torsional graphene-fiber motor. *Adv. Mater.* **26**, 2909-2913 (2014).
20. S. M. Mirvakili *et al.*, Niobium nanowire yarns and their application as artificial muscles. *Adv. Funct. Mater.* **23**, 4311-4316 (2013).
21. S. M. Mirvakili, I. W. Hunter, Fast torsional artificial muscles from NiTi twisted yarns. *ACS Appl. Mater. Interfaces* **9**, 16321-16326 (2017).
22. H. C. Berg, Bacterial flagellar motor. *Curr. Biol.* **18**, R689-R691 (2008).
23. Y. Sowa, R. M. Berry, Bacterial flagellar motor. *Q. Rev. Biophys.* **41**, 103-132 (2008).
24. J. Hollerbach, I. W. Hunter, J. Ballantyne. A comparative analysis of actuator technologies for robotics. In: robtics review 2, 301-345 (MIT Press, Cambridge, MA, 1991).
25. T. Mirfakhrai, J. D. W. Madden, R. H. Baughman, Polymer artificial muscles. *Mater. Today* **10**, 30-38 (2007).
26. Du, H. Y., Lei, X., Xu, Y. Y., Liang, Z. H. & Wang, Y. H. Multi-stimuli induced shape memory effect of polymers based on poly (vinyl alcohol). *Prog. Chem.* **28**, 1648-1657 (2016).

Acknowledgments

We thank Isabelle Ly for SEM images of the fibers.

Author contributions

P.P. and J.Y. conceived and designed the research project. W.N. prepared the wet-spun fibers. J.Y., C.Z. performed the shape memory characterizations. P.M. designed instruments for characterizations of torsional properties of polymer fibers. J.Y., C.Z., K.K., A.L. and P.P. analyzed the data. J.Y and P.P. wrote the paper. All authors discussed the results and commented on the manuscript.

Supplementary Materials

Materials and Methods
Figs. S1 to S14
Table S1
References (27-29)
Movies S1 to S8

Supplementary Materials for

Shape Memory Polymer Fibers for High-Energy Torsional Actuators

Jinkai Yuan*, Wilfrid Neri, Cécile Zakri, Pascal Merzeau, Karl Kratz, Andreas Lendlein, Philippe Poulin*

*Corresponding author. E-mail: yuan@crpp-bordeaux.cnrs.fr, poulin@crpp-bordeaux.cnrs.fr

This PDF file includes:

Materials and Methods
Figs. S1 to S14
Tables S1
Captions for Movies S1 to S4
References (27-29)

Other Supplementary Materials for this manuscript include the following:

Movies S1 to S4

Materials and Methods

1. Materials

Elicarb® single wall carbon nanotubes (SWNTs) are purchased from Thomas Swan UK. Their diameter ranges typically from one nanometer to a few nanometers. The nanotubes are dispersed in aqueous solutions of surfactant polyoxoethylene glycol octadecyl ether (Brij78®). The SWNT and surfactant weight fractions are 0.5% and 1% respectively. The dispersion is homogenized by sonication using a Branson Digital Sonifier®. The graphene oxide (GO) aqueous solution is purchased from the Graphenea Company, Spain. The monolayer content reaches up to 95% and the single layer has a sheet dimension of 2~3 μm. The polyvinyl alcohol (PVA) was purchased from Seppic, France. It has a molecular weight of 195 kg/mol and a hydrolysis ratio of 98%. PVA is dissolved in deionized water to form aqueous solution with a mass concentration of 8% for further wet-spinning different fibers. All the aforementioned materials are used as received.

2. Wet-spun PVA based fibers.

The neat PVA and PVA composite fibers are prepared by using a coagulation process. First, 10g of PVA solution and 8.42g of SWNT dispersion are mixed to form a stable dispersion. This stable dispersion is then continuously injected into a static coagulation bath made of an aqueous saturated solution of Na_2SO_4, which is achieved at 40°C for a concentration of 320g/L of Na_2SO_4. The injection is controlled by a Teledyne ISCO (Lincoln, Nebraska) dosing piston pump at 1 ml/min through a conical spinneret with a diameter of 300 μm at its tip. The coagulated filament forms a fiber in the Na_2SO_4 bath. The fiber is afterwards taken up and drawn into a water bath to be washed. This water bath is an aqueous solution of $Na_2B_4O_7$ at 0.1 wt%. The washing bath allows salt-and water-soluble surfactants to be removed from the fibers. After washing, the wet fiber is dried by IR heating at 80°C and lastly collected onto a winder. The wet-spun PVA-CNT composite fiber has 5 wt% nanotubes.

The mixture of 10g PVA solution and 10.52 g GO solution is used to spin PVA-GO fiber in order to achieve a GO concentration of 5 wt% in the final solid composite fiber. For spinning neat PVA fibers, a diluted 4 wt% aqueous PVA solution is used to be injected to ensure the same viscous of the flow during wet-spinning. Exactly the same protocol is applied to coagulate, wash, dry, and finally collect the PVA-GO and neat PVA fibers as for PVA-SWNT fibers.

To reduce the diameter, the as-prepared fibers are drawn at 150°C up to a tensile strain of 200% using an oven couple to a tensile load instrument Zwick Z2.5/TN1S.

3. Methods

The morphology of as-prepared fibers was observed by a SEM using a field-emission SEM instrument (JEOL 6700FEG) after sputter coating with platinum. The tensile mechanical properties of different fibers are characterized under tensile load using a Zwick Z2.5/TN1S instrument.

The torsional properties and shape memory behaviors of polymer fibers are characterized and performed using a home-made instrument, as shown in **Fig. S2**. The design is inspired by the work of Morton *et al.* (*27*) that deals with the torsional relaxation of textile fibers. The system can be operated in different modes: (i) measuring the torque needed to twist the fiber by a given angle at room temperature or at programming temperatures; (ii) measuring the recovery torque at fixed deformation; (iii) characterizing the full recovery rotation at free load upon reheating the twisted fibers; (iv) measuring the recovery angle against an applied constant torque to determine the

mechanical output as reheating the fibers. The principles for these four operation modes are detailed as follows.

As shown in **Fig. S2**, the system is composed of stepper Motor 1, Motor 2 and a deflection system in between. They are all connected by a sample fiber and a 40-μm diameter tungsten reference fiber. The Motor 1 applies a certain angle of rotation on the sample fiber, while the Motor 2 twists the reference fiber inversely. The inversely applied angle by Motor 2 actually depends on the operation mode and is controlled by a deflection system (**Fig. S10**). In this deflection system, a 5 V voltage is applied between two electrodes at the ends of the copper sulfate aqueous solution bath, in which a needle vertical to the fiber axis is immersed. The needle is mechanically and electrically connected to the tungsten wire. The position of the needle is detected by measuring its voltage with respect to an electrode in the bath. The system acts as a variable resistor which allows the deflection of the tungsten wire to be measured.

The measured voltage signal is sent back to the electronic card of the system so as to determine the frequency and direction of the voltage input for Motor 2 and Motor1, which accordingly determines the rotation speed and direction with accuracy and negligible friction of the needle in the copper sulfate aqueous solution

In Mode i (**Fig. S11**), Motor 1 twists the sample fiber at the bottom end by a given angle θ_1. The top end of the sample fiber connected to the deflection needle therefore tends to rotate in the same direction. But this movement triggers a variation of the electrical potential of the tungsten fiber, which controls the Motor 2. The latter rotates inversely and continuously by an angle θ_2 to keep the deflection needle always at the initial position during the twist of the sample fiber. The torque applied by Motor 2 on the tungsten fiber can be calculated by

$$\Gamma = G_t \frac{\pi R_t^4}{2} \frac{\theta_2}{L_t}$$

where G_t, L_t, and R_t are the shear moduli, length and radius of tungsten fiber, and found to be 161 GPa, 20 cm and 20 μm respectively. This torque is exactly equal to the one applied to the sample fiber by Motor 1. This mode allows for the characterization of the torsional properties of fibers and also for inserting twist at high programming temperatures.

In Mode ii, the twisted deformation of sample fiber is fixed, so Motor 1 does not rotate and fix the bottom end of the sample fiber (**Fig. S12**). While upon reheating, the fiber untwists by rotating the top end of the fiber connected to the deflection needle. This trigger again a variation of the electrical potential of the tungsten fiber, which controls the rotation of Motor 2 by certain angles to keep the deflection needle always at the initial position during reheating the sample fiber. We use the same method in Mode i to calculate the applied torque by Motor 2. This torque is the recovery torque when reheating the twisted sample fiber.

In Mode iii (**Fig. S13**), the load against the rotation of twisted fiber is 0 N.m, so Motor 2 does not rotate and fix the top end of reference fiber. Upon reheating the sample fibers, Motor 1 rotates continuously to ensure that the deflection needle always remains at the initial position (torque is 0 N.m). So the rotation angle of Motor 1 is the recovery rotation of sample fiber during reheating.

In Mode iv (**Fig. S14**), a given applied constant torque Γ is provided by Motor 2 by rotating the deflection needle by a certain angle θ. This angle can be calculated by the equation.

$$\theta = \frac{2\Gamma L_t}{G_t \pi R_t^4}$$

Where G_t, L_t, and R_t are the shear moduli, length and radius of tungsten fiber respectively. Upon reheating the sample fibers, Motor 1 rotates continuously to ensure that the deflection needle

always remains at the same position (angle θ is constant). So the rotation angle of Motor 1 is the recovery rotation of samples against the load Γ during reheating. This mode allows for the measuring the mechanical energy generated by the fiber in rotation.

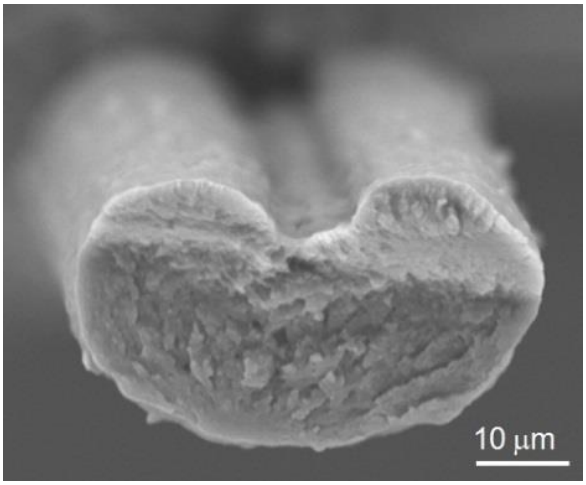

Fig. S1. The cross-sectional SEM image of a PVA fiber. The fiber cross-section has a bean shape. In the following, we assume the fiber as cylinder of radius *R* with the same cross-section area as the actual fiber. The sectional area is measured by the software Imagej. In the present example, the radius of the equivalent cylindrical fiber is ~20 μm.

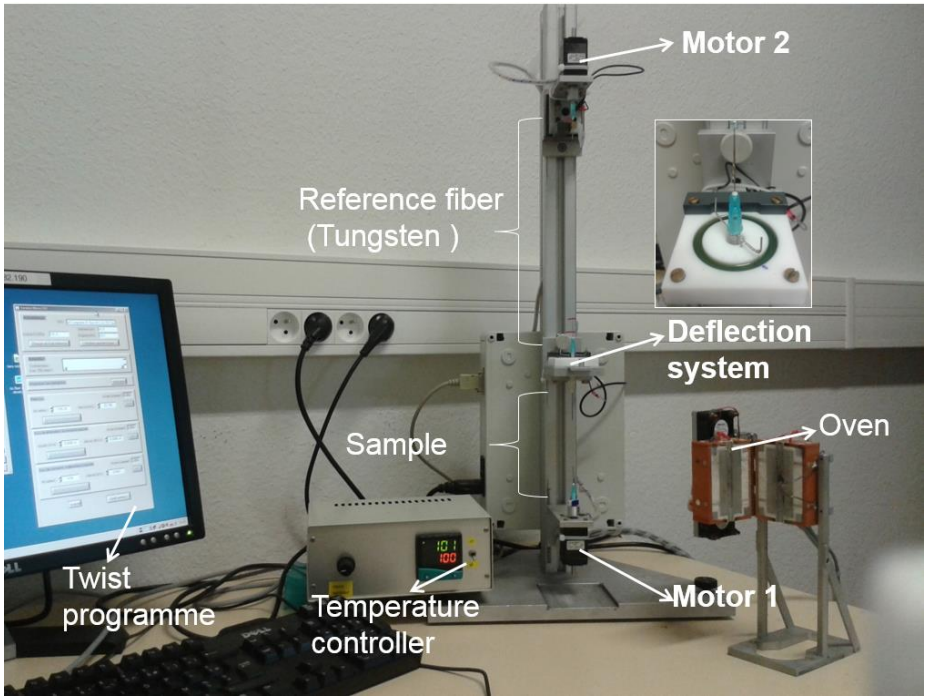

Fig. S2. Home-made instruments. This system includes a small oven with controllable heating rate and a system which measures the torque and angle applied onto a polymer fiber. In particularly, the polymer fibers can be twisted at a high temperatures, T_d. The system can also measure the generated torque, the recovered rotation, and the torsional work capacity of the twisted fibers upon reheating at a given rate.

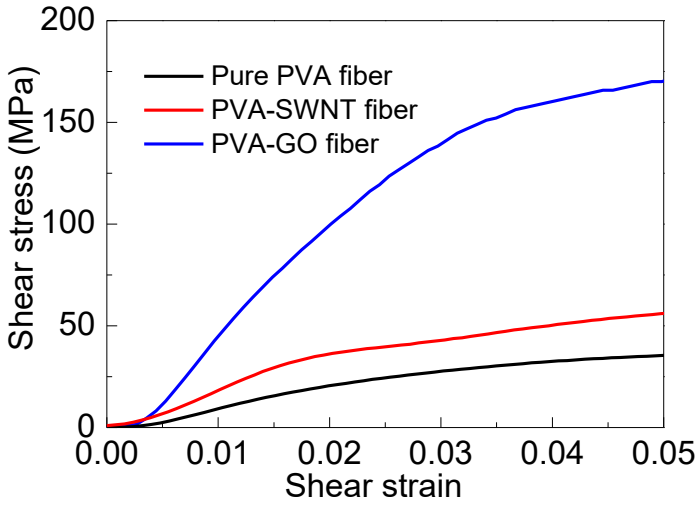

Fig. S3. Shear stress versus shear strain at low twist levels. The shear strain $\gamma_{xy} = R_s \frac{\theta}{L_s}$, the shear stress $\tau_{xy} = \Gamma / (\frac{\pi R_s^3}{2})$, where R_s and L_s are the radius and length of the sample fiber, while Γ and θ are the directly measured torque and twisted angle respectively. The linear fitting of the linear regions of the curves gives shear moduli of 6.8 GPa, 2.3 GPa and 1.3 GPa for PVA-GO, PVA-SWNT and pure PVA fiber respectively.

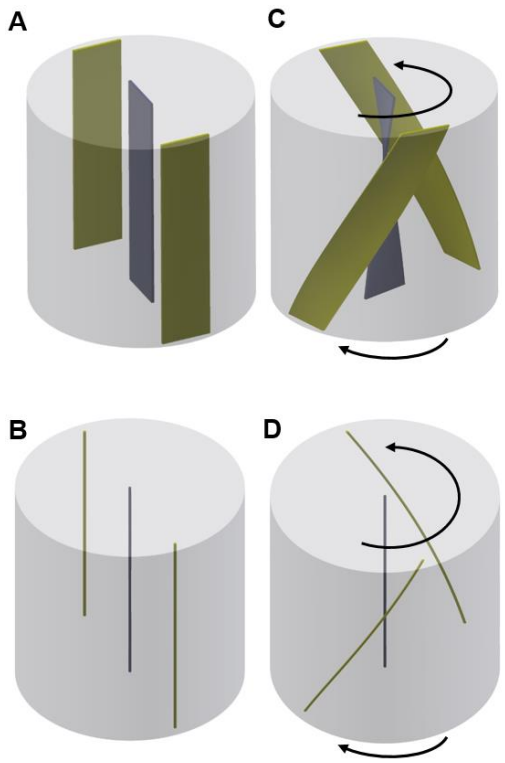

Fig. S4. The schematic image shows how the SWNT and GO nanofillers respond to the applied twisted deformation in different fibers: (**A**) raw PVA-GO fiber, (**B**) raw PVA-SWNT fiber, (**C**) twisted PVA-GO fiber and (**D**) twisted PVA-SWNT fiber.

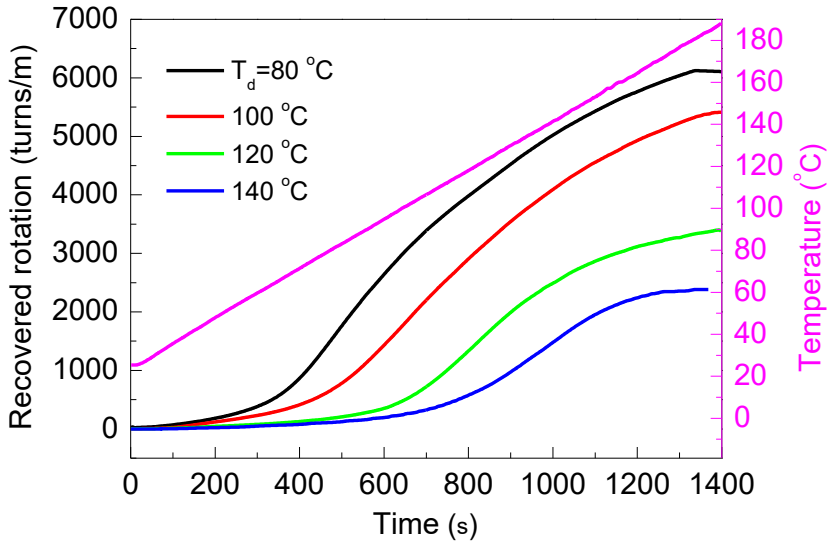

Fig. S5. Recovered rotation with free load for twisted fibers that are programmed at different T_d, upon reheating from room temperature to 185°C at a rate of 5°C/min.

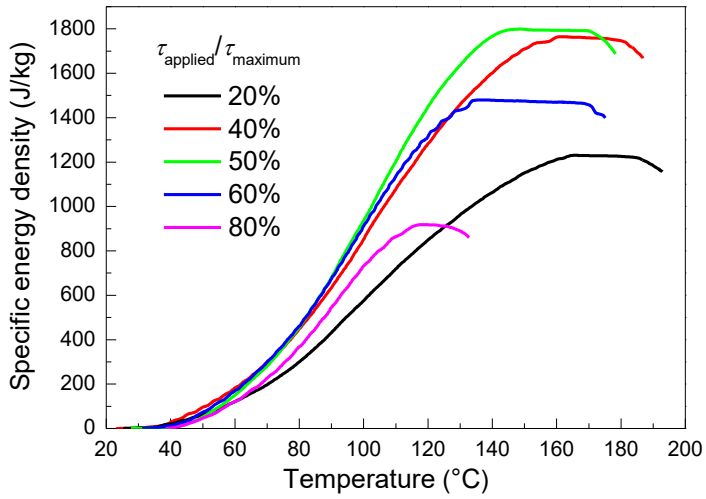

Fig. S6. Gravimetric work capacity of twisted PVA-GO fibers with different loads in response to heating from room temperature to high temperatures. The coiled fibers that have been quenched without being hooked when they are reheated. The percentage indicates the ratio between applied torque and the maximum recovery torque (or blocking torque).

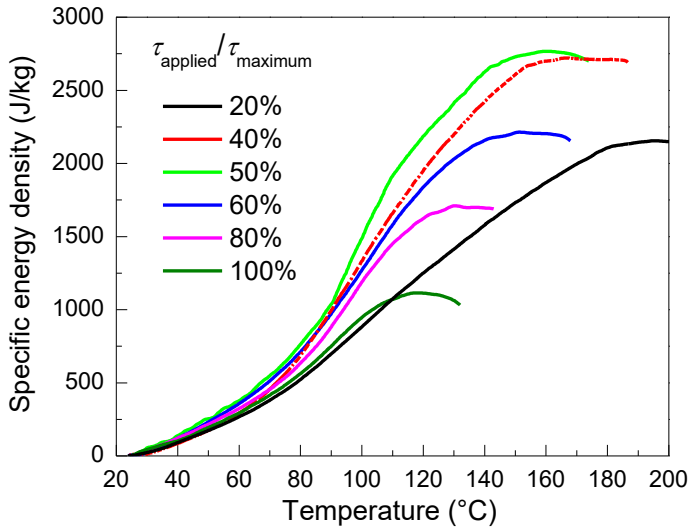

Fig. S7. Gravimetric work capacity of twisted PVA-GO fibers with different loads in response to the heating from room temperature to high temperatures. The coiled fibers are quenched by balancing the twist inserted into the fibers. The hook are removed before being stimulated to rotate. The percentage indicates the ratio between applied torque and the maximum recovery torque (or blocking torque).

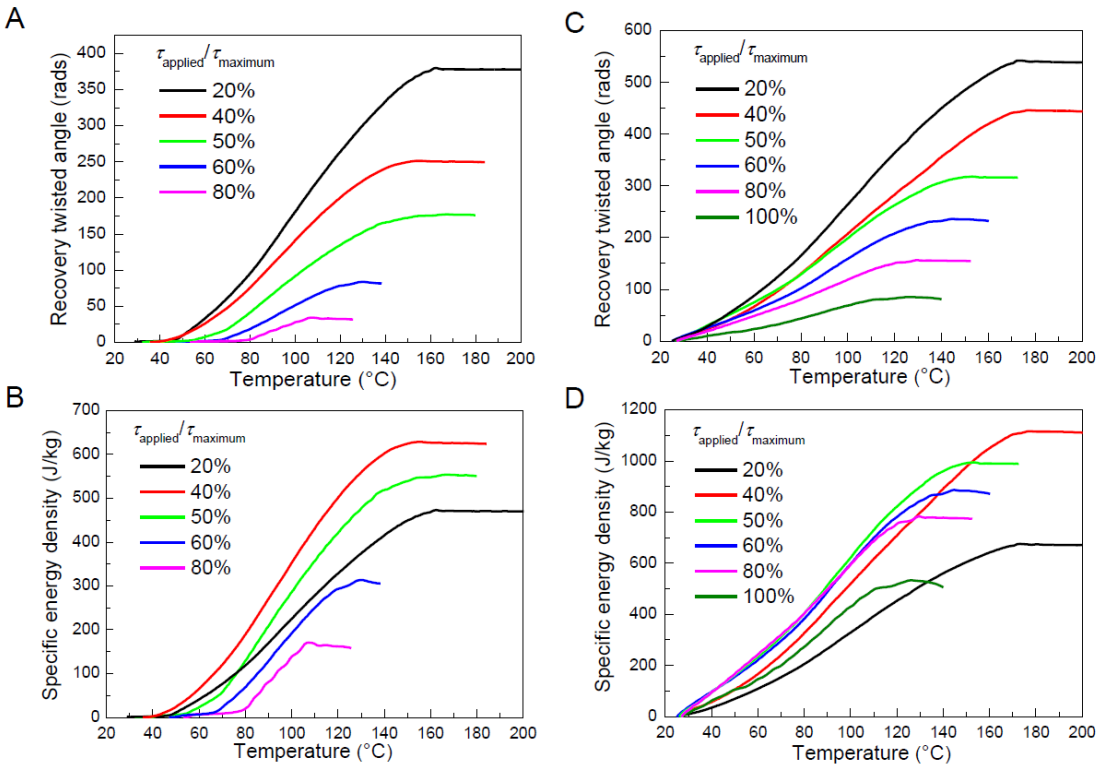

Fig. S8. (**A**) Recovery angle as a function of temperature in conditions of variable applied torques $\tau_{applied}$ for the programmed PVA-SWNT fibers. The applied torque $\tau_{applied}$ varies from 20% to 80% of $\tau_{maximum}$ ~0.12 μN m of PVA-SWNT fiber. (**B**) Gravimetric work capacities for different coiled fibers as a function of temperature. The coiled fibers used for (A, B**)** are formed by quenching in air without being hooked. (**C, D**) The same protocol to measure the recovery angle and gravimetric energy density against a variable constant torque from 20% to 80% of $\tau_{maximum}$ ~0.12 μN m. The only difference is the used coiled fibers are quenched by balancing the twist inserted into the fibers. The hook are removed before being stimulated to rotate.

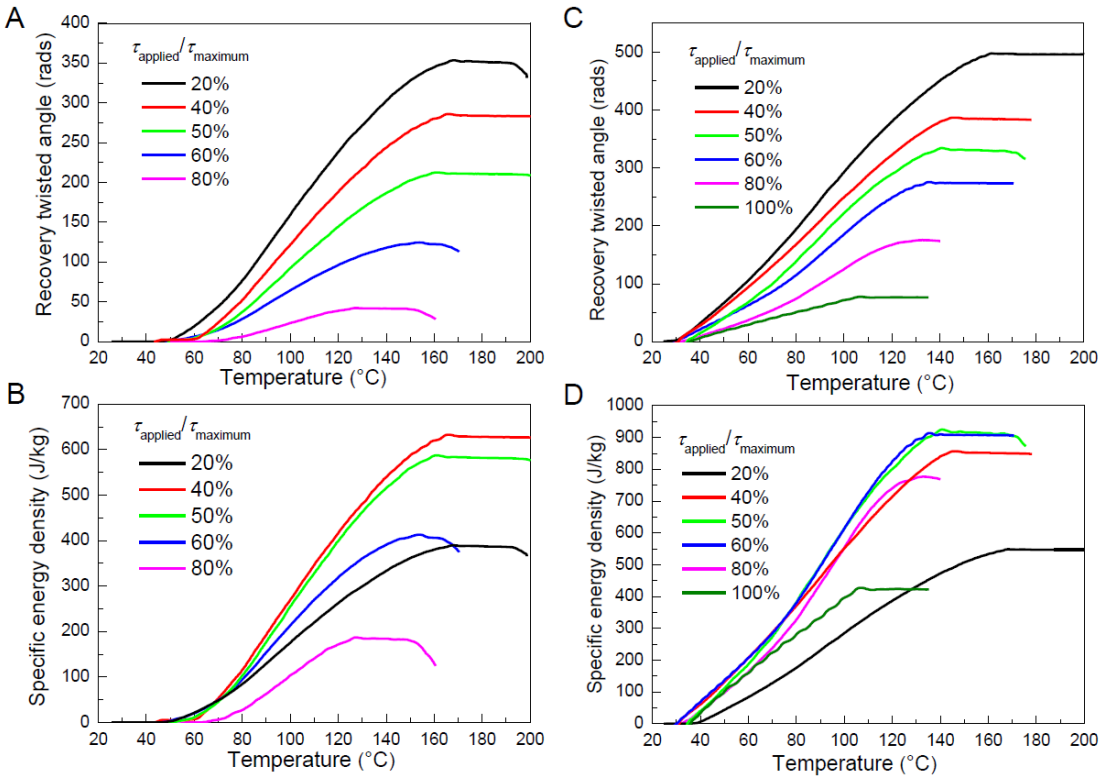

Fig. S9. (**A**) Recovery angle versus temperature at different applied torques $\tau_{applied}$ for the programmed neat PVA fibers. The applied torque $\tau_{applied}$ varies from 20% to 80% of $\tau_{maximum}$ ~0.11 μN m of neat PVA fiber. (**B**) Gravimetric work capacities of coiled fibers as a function of temperature for different loads. The coiled fibers used for (A, B**)** are formed by quenching in air without being torque banlanced. (**C, D**) The same method is applied to measure the recovery angle and gravimetric energy density against a variable constant torque from 20% to 80% of $\tau_{maximum}$ ~0.11 μN m. But the used coiled fibers are quenched by hooking the twisted fibers. The hook are removed before being stimulated to rotate.

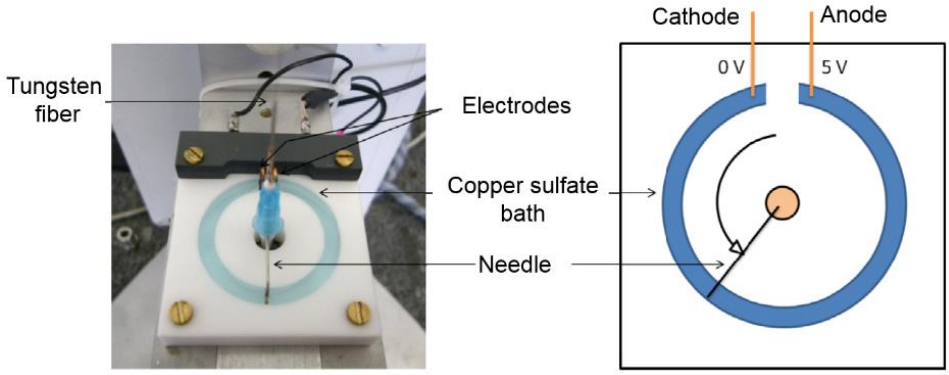

Fig. S10. Photograph and schematic of the deflection system. The system works based on a variable resistor formed by the copper sulfate aqueous solution bath.

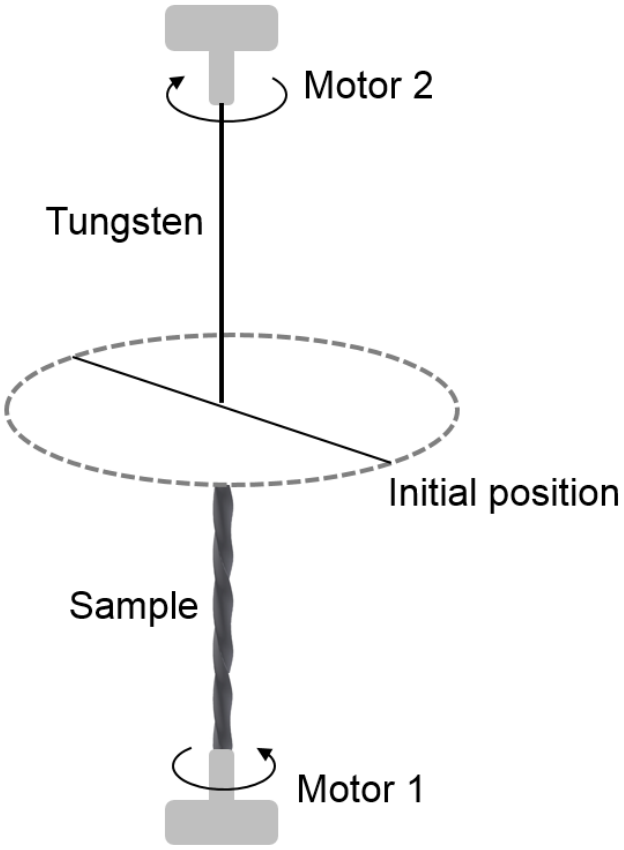

Fig. S11. Schematic image of the system for Mode i.

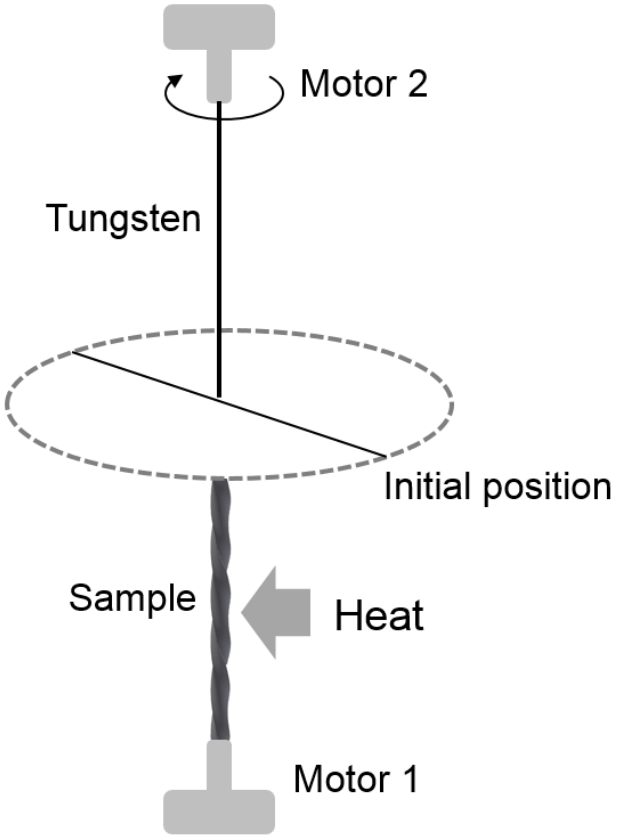

Fig. S12. Image schematically show the operation principle for the system for Mode ii.

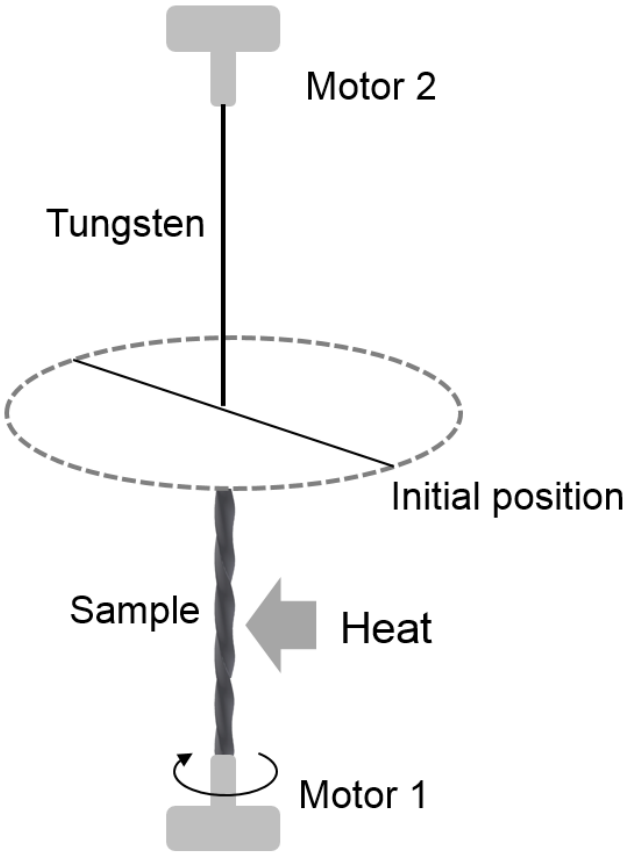

Fig. S13. Operation principle of the system for Mode iii.

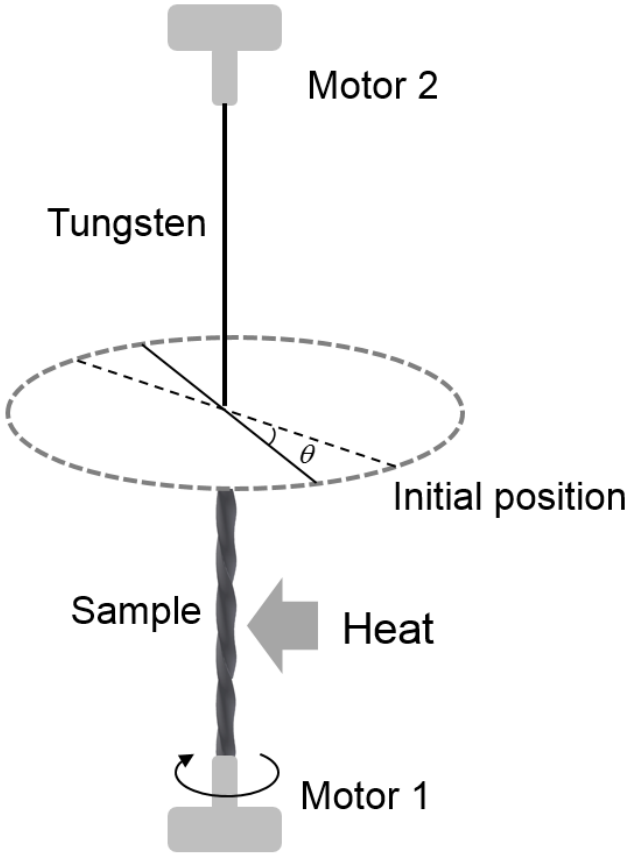

Fig. S14. Operation principle of the system for Mode iv.

Table S1 Comparisons of the torsional performances of different actuators and muscles

Materials	Generated torque (Nm/kg)	Generated rotations (Turns/m)	Rotation Rate (rpm)	Energy density (J/kg)	References
CNT yarn	1.85	694	590	73.2	Ref *7*
Guest filled twist-spun CNT yarns	8.42	43.5	11500	1360	Ref *8*
CNT yarn filled by SEBS polymer and parafin wax	2.21	22	9800		Ref *11*
Helical CNT fibers	0.63	1200	6361	26.7	Ref *12*
Twisted nylon-6,6 fibers	14.4			2100	Ref *14*
GO hydrogel fibers	0.082	1635	5190	230	Ref *19*
Buckled sheath-core fibers		13	2700		Ref *15*
Shape memory NiTi	8	44	10500	0.11	Ref *21*
Niobium nanowire	0.9	33	7200		Ref *20*
CNT yarns		200		0.174	Ref *28*
CNT yarns actuated by water adsorption	0.4	170	700		Ref *13*
Mammalian skeletal muscles				39	Ref *25*
Nature skeletal muscle				47	Ref *29*
Commercial direct drive electric motors	2.5-6				Ref *24*
Shape memory alloy		0.4			Ref *2*
Piezoelectric ceramics		0.022			Ref *3*
Conducting polymers		0.028			Ref *4*
Nature's bacterial flagellar	200				Ref *22, 23*
PVA-GO twisted fibers	21	4467	600	2766	Our work

Captions for Movies S1 to S4

Movie S1
A 4-cm-long, 40-μm-diameter PVA fiber was first inserted a twist of 87 turns with a rotating speed of 240 rpm at 100°C. Then the fiber was quenched at room temperature in air to freeze the twisted deformation. Finally, the fiber untwisted to revert toward its initial shape upon reheating in an oven.

Movie S2
A 3-cm-long, 40-μm-diameter PVA-GO fiber was first programmed by applying a twist of 225 turns at a rotating rate of 60 rpm at 80°C. The fiber was then quenched at room temperature to fix the twisted deformation. Upon immediate heating at 100°C in an oven, the fiber untwists with a peak rotation rate of 600 rpm. One end of the fiber is tethered and the other end is fixed to a 5000 times heavier syringe needle and a paper paddle.

Movie S3
A 3-cm-long, 40-μm-diameter PVA-GO fiber was first twisted by 85 turns at a rotating rate of 60 rpm at 100°C. Then the fiber was quenched at room temperature to freeze the twisted deformation. Upon immersing into 100°C viscous silicon oil, the fiber rotated a 17,600 times heavier rotor composed of a syringe needle and a Teflon paddle.

Movie S4
Five 100-μm-diameter PVA-CNT fibers were plied together to form a yarn with a length of 12 cm, which was then programmed by inserting a twist of 80 turns at a rotation rate of 60 rpm at 100°C. Then the yarn was quenched at room temperature to freeze the twisted deformation. The twisted fiber was shortened to 9.5 cm, and placed under a boat and connected to a spring on one end, and to a propeller on the other end.
The boat with twisted fibers was finally placed in the preheated silicon oil (100°C).

References and Notes

1. G. V. Stoychev, L. Ionov, Actuating fibers: design and applications. *ACS Appl. Mater. Interfaces* **8**, 24281-24294 (2016)
2. K. J. Gabriel, W. S. N. Trimmer, J. A. Walker, A micro-rotary actuator using shape memory alloys. *Sens. Actuators* **15**, 95-102 (1988).
3. J. Kim, B. Kang, Performance test and improvement of piezoelectric torsional actuators. *Smart Mater. Struct.* **10**, 750-757 (2001).
4. Y. Fang, T. J. Pence, X. B. Tan, Fiber-directed conjugated-polymer torsional actuator: nonlinear elasticity modeling and experimental validation. *IEEE-Asme T. Mech.* **16**, 656-664 (2011).
5. J. Yuan, P. Poulin, Fibers do the twist. *Science* **343**, 845-846 (2014).
6. C. S. Haines *et al.*, New twist on artificial muscles. *Proc. Natl. Acad. Sci. U S A.* **113**, 11709-11716 (2016).

7. J. Foroughi *et al.*, Torsional carbon nanotube artificial muscles. *Science* **334**, 494-497 (2011).
8. M. D. Lima *et al.*, Electrically, chemically, and photonically powered torsional and tensile actuation of hybrid carbon nanotube yarn muscles. *Science* **338**, 928-932 (2012).
9. M. D. Lima *et al.*, Efficient, Absorption-powered artificial muscles based on carbon nanotube hybrid yarns. *Small* **11**, 3113-3118 (2015).
10. S. H. Kim *et al.*, Bio-inspired, moisture-powered hybrid carbon nanotube yarn muscles. *Sci. Rep.* **6**, 23016 (2016).
11. K. Y. Chun *et al.*, Hybrid carbon nanotube yarn artificial muscle inspired by spider dragline silk. *Nat. Commun.* **5**, 3322 (2014).
12. P. N. Chen *et al.*, Hierarchically arranged helical fibre actuators driven by solvents and vapours. *Nat. Nanotech.* **10**, 1077-1083 (2015).
13. S. S. He *et al.*, A mechanically actuating carbon-nanotube fiber in response to water and moisture. *Angew. Chem. Int. Ed.* **54**, 14880-14884 (2015).
14. C. S. Haines *et al.*, Artificial muscles from fishing line and sewing thread. *Science* **343**, 868-872 (2014).
15. Z. F. Liu *et al.*, Hierarchically buckled sheath-core fibers for superelastic electronics, sensors, and muscles. *Science* **349**, 400-404 (2015).
16. P. Miaudet *et al.*, Shape and temperature memory of nanocomposites with broadened glass transition. *Science* **318**, 1294-1296 (2007).
17. C. Mercader *et al.*, Scalable process for the spinning of PVA-carbon nanotube composite fibers. *J. Appl. Polym. Sci.* **125**, E191-E196 (2012).
18. M. Behl, M. Y. Razzaq, A. Lendlein, Multifunctional shape-memory polymers. *Adv. Mater.* **22**, 3388-3410 (2010).
19. H. Cheng *et al.*, Moisture-activated torsional graphene-fiber motor. *Adv. Mater.* **26**, 2909-2913 (2014).
20. S. M. Mirvakili *et al.*, Niobium nanowire yarns and their application as artificial muscles. *Adv. Funct. Mater.* **23**, 4311-4316 (2013).
21. S. M. Mirvakili, I. W. Hunter, Fast torsional artificial muscles from NiTi twisted yarns. *ACS Appl. Mater. Interfaces* **9**, 16321-16326 (2017).
22. H. C. Berg, Bacterial flagellar motor. *Curr. Biol.* **18**, R689-R691 (2008).
23. Y. Sowa, R. M. Berry, Bacterial flagellar motor. *Q. Rev. Biophys.* **41**, 103-132 (2008).
24. J. Hollerbach, I. W. Hunter, J. Ballantyne. A comparative analysis of actuator technologies for robotics. In: robtics review 2, 301-345 (MIT Press, Cambridge, MA, 1991).
25. T. Mirfakhrai, J. D. W. Madden, R. H. Baughman, Polymer artificial muscles. *Mater. Today* **10**, 30-38 (2007).
26. Du, H. Y., Lei, X., Xu, Y. Y., Liang, Z. H. & Wang, Y. H. Multi-stimuli induced shape memory effect of polymers based on poly (vinyl alcohol). *Prog. Chem.* **28**, 1648-1657 (2016).
27. W. E. Morton, F. Permanyer. The measurement of torsional relaxation in textile fibers. *J. Text. I. Trans.* **38**, T54-T59 (1947).
28. W. Guo, et al, A Novel Electromechanical Actuation Mechanism of a Carbon Nanotube Fiber, *Adv. Mater.* **24**, 5379–5384 (2012).
29. D. R. Peterson, J. D. Bronzino, Biomechanics: principles and applications (CRC Press, Boca Raton, FL, 2008).